

# On Distinguishing the Multiple Radio Paths in RSS-based Ranging

Dian Zhang<sup>1,2</sup>, Yunhuai Liu<sup>3</sup>, Xiaonan Guo<sup>2</sup>, Min Gao<sup>2</sup> and Lionel M. Ni<sup>2</sup>

College of Software, Shenzhen University<sup>1</sup>

Department of Computer Science and Engineering, Hong Kong University of Science and Technology<sup>2</sup>

Third Research Institute of Ministry of Public Security<sup>3</sup>

{zhangd, guoxn, gao,ni}@ust.hk<sup>2</sup>, yunhuai.liu@gmail.com<sup>3</sup>

**Abstract**—Among the various ranging techniques, Radio Signal Strength (RSS) based approaches attract intensive research interests because of its low cost and wide applicability. RSS-based ranging is apt to be affected by the multipath phenomenon which allows the radio signals to reach the destination through multiple propagation paths. To address this issue, previous works try to profile the environment and refer this profile in run-time. In practical dynamic environments, however, the profile frequently changes and the painful retraining is needed. Rather than such static ways of profiling the environments, in this paper, we try to accommodate the environmental dynamics automatically in real-time. The key observation is that given a pair of nodes, the RSS at different spectrum channels will be different. This difference carries the valuable phase information of the radio signals. By analyzing these RSS values, we are able to identify the amplitude of signals solely from the Line-of-Sight (LOS) path. This LOS amplitude is a simple function of the path length (the physical distance). We find that the analysis is a typical non-linear curvature fitting problem that has no general routing algorithms. We prove this problem format is ill-conditioned which has no stable and trustable solutions. To deal with this issue, we further explore the practical considerations for the problem and reform it to a greatly improved conditioning shape. We solve the problem by numerical iterations and implement these ideas in a real-time indoor tracking system called MuD. MuD employs only three TelosB nodes as anchors. The experiment results show that in a dynamic environment where five people move around, the averaged localization error is 1 meter. Compared with the traditional RSS-based approaches in dynamic environment, the accuracy improves up to 10 times.

## I. INTRODUCTION

Ranging plays an essential role in indoor localizations [2], [12], [11], [4]. Among the various techniques, one promising approach is based on Radio Signal Strength (RSS). Nodes simply measure the packet RSS in between and map the RSS values to the corresponding distances. Compared with other ranging techniques, RSS-based ranging offers many unique advantages. It requires little hardware support and can be applied with any wireless transceivers, making the RSS nearly a free resource for ranging. Therefore, RSS-based ranging (localizations) has attracted a vast amount of research efforts.

As RSS measurement is easy and convenient, the mapping from RSS to distances is the key issue. In theory, this mapping is a unique and monotonous function. For example, the free-space path loss model [14] suggests that the RSS path loss is proportional to the square of the distance. In practice,

however, this model is far from reality. It has been well known that the function is a dynamic, complex one that depends on many factors [14]. The most significant one is the multipath propagation phenomenon [2], which refers to the radio propagation nature that radio signals reach the receiver by two or more physical paths. The causes are many such as the atmospheric duct, refraction and reflection. Signals from different paths combine at the receiver constructively or destructively depending on signal phases. As the phases are environment-dependent, the RSS of combined signals is very sensitive to the environment changes. Fig. 1 depicts some real RSS measurements for a pair of TelosB nodes [1] under different distances in different environments. At each node distance, the bar shows the RSS difference at different places. Apparently there has no simple unique function between the RSS and the corresponding distance.

To find an appropriate mapping between the RSS and the distance, a lot of research works have been conducted. Their fundamental way is to profile the radio environment and refer the profile when ranging. Representative works include the RADAR [2], statistic approaches [15], and etc. [12], [11], [4]. Profile-based approaches require a labor-intensive training procedure to provide the environment profile, which is too costly and becomes practically infeasible when the environment changes fast (e.g., people moving around).

Revisiting the multipath effect, we argue that a more fundamental way to deal with the issues is to accommodate the environmental dynamics in real time. We attempt to distinguish the signals from different paths, filter out signals from the Non-Line-Of-Sight paths (NLOS) and identify the one from the Line-Of-Sight path (LOS). As such the multipath effect can be canceled. We stem only on the RSS values and requires no additional hardware support or lower-layer protocol information. To the best of our knowledge, this is the first work in literature towards this goal with such constraints.

This goal is extremely difficult due to the limited information of RSS. RSS measures only the signal amplitude and provide no signal phase information. Signals from different paths may exhibit similar behaviors from the RSS's perspective. RSS of a distant LOS path may be exactly the same as that of a close but reflected path. Moreover, using commodity hardware, we have no direct observations on the NLOS paths.

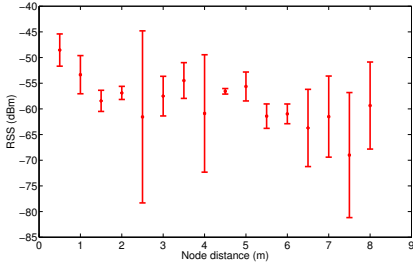


Fig. 1. RSS measurement in different environments

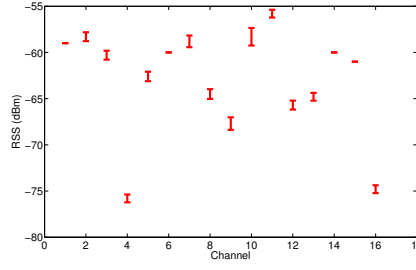


Fig. 2. RSS measurement in different channels: node distance=2m

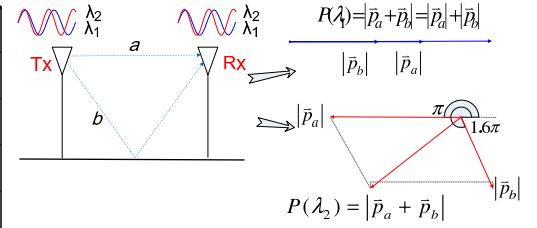


Fig. 3. An illustrative example; there are two paths  $a$  and  $b$ ; The signals of two frequencies  $\lambda_1, \lambda_2$  will have different RSS values at the receiver end because of the phase-shift difference between paths (i.e.,  $P(\lambda_1) \neq P(\lambda_2)$ )

An interesting observation is that the frequency diversity may help RSS provide phase information indirectly. Fig. 2 depicts some RSS measurements at the same environment for a pair of TelosB sensors [1] at different spectrum channels (the band is divided into 16 channels). We can see that, the pair of nodes may have significantly different RSS values at different spectrum channels and the measurements are quite stable at the same environment. This RSS difference at different channels is essential for our work as it carries the valuable phase information. By carefully analyzing these RSS, we can identify the amplitudes and phases of signals from each path, then derive the accurate distance according to the amplitude of LOS signals. A clearer illustrative example is in Sec. 2.3.

We find that the analysis of RSS values is a typical non-linear curvature fitting problem with trigonometric model functions. It has no close-form solutions and is typically approximated by numerical iterations. We also find that the original fitting problem has a bad shape. Its Hessian matrix is ill-conditioned and the solutions will be un-stable and not trustable, which may yield great ranging errors. To deal with this issue, we further explore the practical considerations to reform the problem. For example, certain hardware-dependent parameters, though unknown, will be unlikely to change and can be obtained before ranging. The LOS path is always the shortest path, and reflection will absorb a lot of signal energy. Granting these facts, we design treatment techniques to the problem. Thus, the reformed problem has greatly improved conditioning and the solutions become much more stable.

To demonstrate the effectiveness of the ideas, we implement a real tracking system called MuD (Multipath Distinguishing). It is based on TelosB [1] platform. Compared with traditional RSS-based ranging (localization), MuD offers the following key advantages. 1) It is robust to the environment dynamics. Moving people, new furniture and etc. will not degrade its performance unless the LOS path is affected (e.g., blocked); 2) No labor-intensive training is needed. The training of hardware-oriented parameters is a one-time operation and can be done in an online manner. We can also use values in the hardware specification manual to assign these parameters. It will sacrifice about 10% accuracy; 3) Ranging in MuD is very accurate in dynamic environments. Therefore three anchor nodes for trilateration purposes are enough for localizations. Experimental results show that the average ranging

(localization) error is about 1 meters in complex and dynamic environments (five people moving around). Compared with the traditional RSS-based approaches in dynamic environment, the accuracy is improved by 10 times.

The rest of this paper is organized as follows. In Sec. 2, we will give some background information. Sec. 3 will give the system model and the problem definition. Sec. 4 will show how to use non-linear optimization to solve the above problem. Sec. 5 presents the our treatment techniques to improve the problem conditioning. We will describe the implementation of MuD tracking system and evaluate its performance in Sec. 6. Sec. 7 will be the related work. We will conclude this work and point out our future work in the last section.

## II. MULTIPATH EFFECT AND FREQUENCY DIVERSITY

In this section, we first introduce the background of the radio propagations in free space, then describe how the signal behaves in multipath phenomenon. At last we use a simple example to illustrate how to exploit the frequency diversity to cope with the multipath effects.

### A. Radio Propagation in Free Space

Radio propagation describes the behavior of radio waves when they are transmitted from the transmitters to the receivers. During the propagation, radio waves will fade out with the distance. By Friis model [14] it can be expressed as

$$|\vec{p}| = \frac{P_t G_t G_r \lambda^2}{(4\pi d)^2} \quad (1)$$

where  $\vec{p} = \{|\vec{p}|, \theta\}$  is the signal wave vector,  $|\vec{p}|$  is its amplitude and  $\theta$  is its phase at the receiver,  $P_t$  is the transmission power,  $G_t, G_r$  are the antenna gain of the transmitter and receiver,  $\lambda$  is the signal wavelength and  $d$  is the LOS path length between the transmitter and receiver. Suppose the sender has the phase zero, the signals phase at the receiver is

$$\theta = \left(\frac{d}{\lambda} - \lfloor \frac{d}{\lambda} \rfloor\right) \cdot 2\pi \quad (2)$$

In the remainder of this paper, we call  $|\vec{p}|$  the *path strength*, and  $\theta$  the *path phase*. For signals along the LOS path, the Friis model is appropriate to describe its behavior as there is no other fading. For NLOS paths in a multipath scenario, we need more physical laws.  $\lfloor \cdot \rfloor$  is the floor operator.

### B. Multiple NLOS Paths

The NLOS paths between the transmitter and receiver are mainly induced by reflection and refraction. Reflection refers to a radio propagation phenomenon that changes in direction of the signal waves at an interface between two different media. It results in the returned wave to the original medium. In the indoor environments, the reflections typically occur at the surface of the objects, walls, and the ground. In each reflection, partial energy will be transmittance, partial will be reflectance and the left will be absorbed by the medium. The reflectance part is measured by the *reflection coefficient*  $\Gamma$  which is the ratio of the strength of the reflected radio wave  $E^-$  to the strength of the incident wave  $E^+$ , i.e.,

$$\Gamma = \frac{E^-}{E^+} \quad (3)$$

With (1) and (3), for a given NLOS path, its path strength is

$$|\vec{p}| = \Gamma \frac{P_t G_t G_r \lambda^2}{(4\pi d)^2} \quad (4)$$

Notice that  $d$  is the length of NLOS path and this time it is not equal to the distance between the transmitter and receiver. The expression of path phase is similar to (2).

Refraction is another source of the NLOS paths. It has similar effect on the path strength while this time the transmittance part of the energy rather than the reflected part will be received by the receiver. The path phase is the same as (2).

According to these physical properties, given a pair of nodes in a static environment, when signals of one channel propagate along a set of paths, very likely the signals of a nearby channel will propagate along the same set of paths. It is because the reflection and refraction are mainly characterized by the wavelength of the signal and nearby channels have a similar wavelength. For example, TelosB nodes [1] work on 2.4G band to 2.4835G band. The wavelengths are 0.125m to 0.1208m. The difference is only 4.7 millimeters. Thus, unlikely will the existing paths disappear or new paths emerge.

### C. Motivation Example

We also notice that for each path, its path phase will change when the signal frequency changes. For the example in Fig. 3, suppose the path  $a$  is two meters. The 2.4G signals will have the path phase  $\theta_a(\lambda_1) = (\frac{d_a}{\lambda_1} - \lfloor \frac{d_a}{\lambda_1} \rfloor) \cdot 2\pi = (\frac{2}{0.125} - \lfloor \frac{2}{0.125} \rfloor) \cdot 2\pi = 0$ . The 2.48G signal has the path phase  $\theta_a(\lambda_2) = (\frac{2}{0.1208} - \lfloor \frac{2}{0.1208} \rfloor) \cdot 2\pi = \pi$ . The changed path phase, called *phase-shift* with respect to the path  $a$  is  $\Delta\theta_a = \theta_a(\lambda_2) - \theta_a(\lambda_1)$ . The phase-shift depends on the path length  $d$ . It is not directly measurable by commodity hardware.

A key observation to motivate this work is that we can measure the consequence of this phase-shift (the different RSS (Fig. 2) at different channels), and infer the phase-shift by analyzing these different RSS. More specifically, suppose another path  $b$  in Fig. 3 is three meters. Its phase-shift will accordingly be  $\Delta\theta_b = \theta_b(\lambda_2) - \theta_b(\lambda_1) = 1.6\pi$ . The phase-shifts with respect to different paths are different ( $\Delta\theta_a \neq \Delta\theta_b$ ). These different phase-shifts will change the

constructive and destructive relations between signals from different paths. In Fig. 3, at  $\lambda_1$ , the signals from  $a$  and  $b$  are completely constructive, and at  $\lambda_2$ , the signals from the two paths become somehow destructive. This changed relation will result in a changed RSS measurement. As there are a limited number of paths, and each path introduces a limited number of unknown parameters, we can solve all the unknowns with a sufficient number of RSS measurements at different channels. Indeed, as we will show later, each path will introduce two new unknowns. The current 2.4G Zigbee compliance supports up to 16 channels, and therefore it can accommodate up to 8 paths between the transmitter and receiver.

## III. PROBLEM DEFINITION

The basic idea of our RSS-based ranging is to let nodes collect the RSS measurements of different spectrums, then make a calculation based on these measurements. In this section we first introduce the system model, then formally define the problem.

### A. System Model and Assumptions

We assume transmitters and receivers are free to dynamically adjust their frequency in run time. This function is supported by most products. Each pair of transmitter and receiver are well coordinated and synchronized.

For a given pair of transmitter  $u$  and receiver  $v$ , suppose there are  $n$  radio propagation paths in between ( $n$  is unknown). Without loss of generality, let the first path be the LOS one and others are NLOS. The path length of these data paths are denoted as  $d_i, i = 1, \dots, n$  (an accurate  $d_1$  is our ultimate goal). The reflection co-efficiency of paths are denoted as  $\Gamma_i$  ( $\Gamma_1 = 1$  for LOS path and others are smaller than 1). Suppose by hardware constraint we can measure up to  $m$  channel RSS and the wavelengths of these channels are  $\lambda_j, j \in [1, m]$ . Given the wavelengths  $\lambda_j$  of one channel, we denote the  $i$ -th path strength as  $p_i(\lambda_j), i \in [1, n]$  and the  $i$ -th path phase as  $\theta_i(\lambda_j), i \in [1, n]$ . During the measurement, we will use the same transmission power  $P_t$  (though again it is unknown). For the given pair of transmitter and receiver, the antenna gain  $G_t$  and  $G_r$  will be fixed. We can substitute all the constants  $P_t, G_t$  and  $G_r$  in (4) by a single one  $c = \frac{P_t G_t G_r}{(4\pi)^2}$ . Thus we have the  $i$ -th path strength as

$$p_i(\lambda_j) = \frac{\Gamma_i c \lambda_j^2}{d_i^2} \quad (5)$$

and the path phase

$$\theta_i(\lambda_j) = (\frac{d_i}{\lambda_j} - \lfloor \frac{d_i}{\lambda_j} \rfloor) \cdot 2\pi \quad (6)$$

Considering the different path phases, the aggregated signal at the receiver is a vector summation. Given wavelength  $\lambda_j$ , the RSS the amplitude of the combined signal is

$$\begin{aligned}
P(x, \lambda_j) &= \left| \sum_{i=1}^n \vec{p}_i \right| \\
&= \left( \left( \sum_{i=1}^n c \lambda_j^2 d_i^{-2} \sin(d_i \lambda_j^{-1}) \right)^2 \right. \\
&\quad \left. + \left( \sum_{i=1}^n c \lambda_j^2 d_i^{-2} \cos(d_i \lambda_j^{-1}) \right)^2 \right)^{\frac{1}{2}} \quad (7)
\end{aligned}$$

Here we apply the orthogonal decomposition method to calculate vector summations. Equ. (7) is a function  $P(x, \lambda_j) : \mathbb{R}^{2n} \rightarrow \mathbb{R}$  with  $x = (c, \Gamma_2, \dots, \Gamma_n, d_1, \dots, d_n) \in \mathbb{R}^{2n}$  be the vectors of unknown parameters, or simply the unknowns. By tradition  $\mathbb{R}$  is the set of real numbers.

### B. Problem Definition

For each  $j$ -th channel, we will have a RSS measurement  $P_j, j \in [1, m]$ . Our main task then becomes to fit these  $m$  measurements  $(\lambda_j, P_j)$  with the *model function*  $P(x, \lambda_j), x \in \mathbb{R}^{2n}$ . We need to find  $x$  so that the fit is as close as possible to the real measurements  $P_j$ . We define the “closeness” of the fitting as the least square, and other norms of vectors are also possible when they are well justified. Formally, the problem is defined as **Curvature Fitting Problem (CFP)**:

given  $r_j(x) : \mathbb{R}^{2n} \rightarrow \mathbb{R}, j = 1 \dots m$

$$\min_{x \in \mathbb{R}^{2n}} f(x) = \frac{1}{2} \sum_{j=1}^m r_j(x)^2 \quad (8)$$

where  $r_j(x) = P(x, \lambda_j) - P_j (j = 1, \dots, m)$  are the individual fitting error,  $P(x, \lambda_j)$  is model function defined in (7).

As long as the problem is solved, the solution, denoted as  $x^*$ , will contain our target  $d_1$ .

## IV. NON-LINEAR OPTIMIZATIONS TO SOLVE CFP

In this section, we will show that the present CFP is not in a good shape and has no trustable and stable solutions by its current form. In the next, we will first present the intuition of this claim based on the concepts of condition number, then present the general method of solving non-linear equations for CFP. In the last we will show that the solution for the current CFP is based on ill-conditioned matrix.

### A. Condition Number of Ill-conditioned Matrix

The intuition of this claim is that, the model function  $P(x, \lambda)$  are managed by parameters co-efficiency  $c$  and path length  $d_i$ . Roughly speaking, the trigonometric part (i.e., sines and cosines) in  $P(x, \lambda)$  “oscillates” the function value and can be considered as a scalar between 0 and 1. The  $\frac{c}{d_i^2}$  portion controls the amplitude and is the dominance part. However, these two parameters  $c$  and  $d_i$  jointly control the function value and will cancel the effects of each other. For example, a doubled estimation of  $d_i$  will cancel the effect of a four time  $c$ , resulting a similar function value.

Mathematically, such situations are called *ill-conditioned* and its degree of the condition is measured by the *condition number*. A high condition number means, a small change in the input will result in a large change in the solution. For instance, a matrix of condition number 100 will have 100% changes on the solution when the input changes 1%. Solutions based on this high condition number matrix can hardly be trusted as there are always certain errors on the input in practice.

### B. General Method for Non-linear Minimizations

In this subsection, we provide some general information of solving non-linear minimizations for CFP. More details can be found in multivariable calculus references [7]. in CFG, the solutions exists only when  $m \geq 2n$ , the unknowns  $x \in \mathbb{R}^{2n}$  are no more than  $m$  model function equations.

**Lemma:** Let  $f : \mathbb{R}^{2n} \rightarrow \mathbb{R}$  be continuously differentiable in an open convex set  $D \in \mathbb{R}^{2n}$ . Then  $x \in D$  can be a local minimizer of  $f$  only if  $\nabla f(x) = 0$ , here  $\nabla f(x) = [\frac{\partial f}{\partial x_1}(x), \dots, \frac{\partial f}{\partial x_{2n}}(x)]^T$ .

**Theorem:** Let  $f : \mathbb{R}^{2n} \rightarrow \mathbb{R}$  be twice continuously differentiable in the open convex set  $D \in \mathbb{R}^{2n}$ , and assume there exists  $x \in D$  such that  $\nabla f(x) = 0$ . if  $\nabla^2 f(x)$  is positive definite, then  $x$  is a local minimizer of  $f$ .  $(\nabla^2 f(x))_{ij} = \frac{\partial^2 f(x)}{\partial x_i \partial x_j}, i \leq 2n, j \leq 2n$

According to these Lemma and Theorem, the essential of CFP is to solve the equations  $\nabla f(x) = 0$  or equivalently,

$$\frac{\partial f}{\partial x_i}(x) = 0, i = 1, \dots, 2n. \quad (9)$$

among all the solutions to find the one with the minimal  $f(x)$ .

Since the model function  $P(x, \lambda_j)$  involves trigonometric function, (8) are non-linear equations. We can find only approximation solutions and there will be unlikely routine algorithm to solve it. This is mainly due to the classical results of no close-form solutions for such problems. Typically the solutions are approximated by numerical iteration. We start the iteration from an initial guess, say  $x^{(0)}$ , construct a local model for the target function and calculate a new guess, say  $x^{(1)}$ . The iteration continues until certain criteria are satisfied, e.g., the number of iterations exceeds a given threshold or the consequent approximations are close enough, say  $\|\nabla f(x^{(k)})\| \leq \varepsilon$  for an arbitrarily small number  $\varepsilon$ . This final iteration approximate is then the solution, i.e.,  $x^* = x^{(k)}$ .

### C. Ill-conditioned Matrix

Applying the Newton’s method to (9) we have the iteration equation  $x^{(k+1)} = x^{(k)} - (\nabla^2 f(x^{(k)}))^{-1} J(x^{(k)})^T R(x^{(k)})$ , where  $J(x) \in \mathbb{R}^{m \times 2n}$  is the Jacobian matrix of  $f$ ,  $J_{ji}(x) = \frac{\partial f}{\partial x_i}(\lambda_j), j = 1, \dots, m; i = 1, \dots, 2n$  and  $H(x) = \nabla^2 f(x)$  is the second derivatives  $H(x) = \sum_{j=1}^m (\nabla r_i(x) \cdot \nabla r_i(x)^T + r_i(x) \cdot \nabla^2 r_i(x))$ . As the general form of  $f$  is too complex that the analytic derivatives  $J(x)$  and  $H(x)$  are hardly to be available, we just give an analysis on the simplest case where  $n = 1$  and  $m = 2$  (only the LOS path). We will show that even for this simplest case the problem may still be ill-conditioned.





Fig. 4. Chamber environments

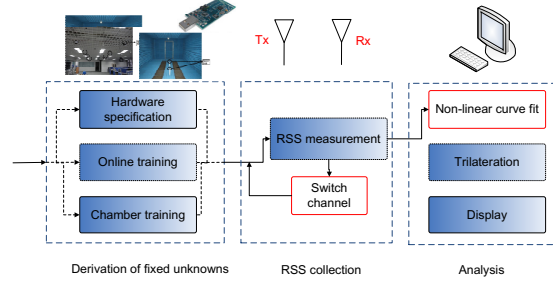


Fig. 5. Architecture of MuD with three major steps: derivation of the fixed unknown  $c$ , RSS collection and analysis

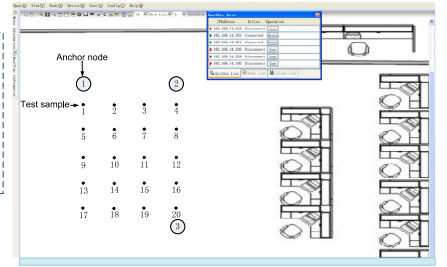


Fig. 6. A snapshot of RSS Experiment environment

**Theorem:** the condition number of Hessian matrix  $\nabla^2 f$  with  $m = 2$  and  $n = 1$  is  $(\frac{9c^2}{d^2} + 4)^2$ .

We omit the proof part because of the page limitation. Based on the theorem, we have the following observation. For the original format of CFP, the condition number can be arbitrary high when  $\frac{c}{d}$  is high enough. For the NLOS paths, we will have a similar conclusion by substituting the product of  $c$  and  $\Gamma_i$ . However, when we can give a tight bound of these parameters, the condition number can be low, making the matrix well-conditioned and the solutions trustable.

## V. TREATMENTS OF PROBLEM

In this section, we will present some practical treatments to solve CFP. We first introduce the basic idea of the treatment techniques, then describe them in details.

### A. Basic Idea of Treatments

By the previous section, we find the original CFP can hardly be solved in its current form because of multiple local optimal solutions in the target function  $f$ . In addition, the analytic form of the iteration equations is too complex to derive, making the iteration quite hard. This is in particular true for scenarios of more paths, say  $n = 8$ . Though mathematicians have their means for such situations, their treatments are often investigated in a case-by-case manner. There are no simple and effective general-purpose methods to do so.

Rather than those purely mathematic ways, in this paper we attempt to address the issue by practical considerations. Observing the model function  $P(x, \lambda)$  in (7), we find the difficulties of the problem from three facts. First, the parameter  $c, \Gamma$  and  $d$  are jointly affecting the function value. The effect of varying one parameter can be canceled by varying the other two parameters for a path. Second, the model function (7) is symmetric in terms of the different paths. We may find the parameters  $c$  and  $d_i$ , but can hardly identify which parameters belong to the LOS by merely the solution. Additional information is needed to identify these parameters. Third, the number of paths  $n$  is critical to the problem complexity. To accommodate one more path, we have two more unknowns ( $\Gamma$  and  $d$ ), need at least two more RSS measurements, and two more nonlinear equations. Too complex iteration equations

may also aggravate the computation errors due to limited computer precisions. The computation will be greatly simplified if we can limit the number of paths  $n$  in calculation, though  $n$  indeed is determined by the environments. In the next, we will present how to exploit these observations to simplify CFP.

### B. Derivation of Fixed Unknowns

A first treatment technique of the problem is to derive some unknowns in the model function. In the model function  $P(x, \lambda)$  (Equ. (7)),  $c$  represents the co-efficiency  $\frac{P_t G_t G_r}{(4\pi)^2}$ . For a given pair of transmitter and receiver and a fixed transmission power,  $c$  will be a constant unknown. We can apply  $c$  to the model function, which will dramatically improve the conditioning of the CFP. So we propose three methods to estimate  $c$  before the run-time ranging, namely by hardware specifications, by chamber training, and by online training.

1) *Hardware Specification Manuals:* Recall the definition of the unknown  $c$ , it is determined by the transmission power  $P_t$ , and antenna gains of the transmitter  $G_t$  and receiver  $G_r$ .  $P_t$  can be transferred from the power level setting in transmission (e.g.,  $1\text{dbm} \approx 1.26\text{mw}$ ), and  $G_t$  and  $G_r$  can be obtained from the hardware specification manual (e.g., use the parameter from TelosB datasheet and use the common approach to estimate the gain of omnidirectional antenna [16], [3]). Though this method provides a poor estimation on  $c$ , it is the simplest one and sets a baseline for comparisons.

2) *Chamber Training:* Chambers are enclosures for researchers to investigate the radio propagation phenomenon. It contains pyramidal absorber materials in the ceilings, walls and ground to absorb the addition radio waves, making it an ideal open space where the Friis model is valid. Fig. 4 shows the chamber that we use in our experiments. As the path length is available, there is only one unknown in the model function  $P(x, \lambda)$ . Thus for a given pair of transmitter and receiver and the fixed transmission power, we can calculate  $c$  by a single RSS measurement. Chamber is an ideal environment and we set it as the upper limit of the accuracy. In practice, the chamber is often too bulky and may not always be available for simple ranging and localization applications.

3) *Online Training:* In practical environments, a more attractive option to obtain the parameter  $c$  is by online manner.

Specifically, initially the transmitters and receivers will be placed at given positions. With known  $d_1$ , we can apply the general method in Sec. 4 to obtain the other unknowns which include  $c$ . During the later run-time, we apply this  $c$  for calculations. Online training is quite convenient as it requires no chamber equipment. The training procedure shares the same environment as the later ranging and localization procedures, though certain degree of the accuracy will be sacrificed. We will evaluate these approaches in later sections.

### C. Reducing the Model Path Number

Another critical parameter in the model function  $P(x, \lambda)$  is the number of paths  $n$ . It will determine the fundamental form of the function. This parameter is fully environment-dependent and can be any, and thus brings great challenges to solve CFP.

Nevertheless, in real environments, some practical considerations allow us to set a conservative  $n$  (say  $n = 5$ ) without sacrificing too much ranging accuracy. First, NLOS paths with three or more reflections or refractions can be ignored. Recall that after each reflection and refraction the path strength will fade according to the reflection co-efficiency  $\Gamma$ . For typical materials,  $\Gamma$  is around 0.5 or less depending on the directional property of the surface [10]. In other words, each reflection or refraction consumes more than 50% of the energy received by the receiver. Three or more reflections on a single NLOS path will consume more than 87.5% of the energy. With over 87.5% of loss on its energy, signals from more than three reflections can be ignored in the model function to simplify the CFP complexity, while it sacrifices some accuracy. Second, we can also ignore the paths which are extremely long, say more than two times of the LOS path. Recall the Friis model in (1), the energy will fade inversely proportional to the square of the path length. A NLOS path more than twice of the LOS one can have the strength at most one fourth. Considering the further impact of reflection/refraction ( $\Gamma$ ), the path energy will be no more than  $0.25 \times 0.5 = 0.125$  of the LOS path energy.

Because of these considerations, we set a relatively small  $n$  in the model function  $P(x, \lambda)$ , say  $n \leq 5$ . Apparently certain accuracy on ranging will be sacrificed. In later we will use experiments to evaluate the parameter  $n$ .

### D. Bounding the Unknowns for NLOS Paths

Another important issue is the initial value of iterations when solving CFP. Basically, Newton's method is quite effective when the initial setting is close to the solution enough. Owing to this property, we are motivated to find the upper bound and lower bound of the unknowns. As the target is continuously tracked, the position displacement of the target will not be large due to the limited mobility in the indoor environments. So we heuristically set the upper bound and lower bound of the new  $d_1$  as the original one plus  $\pm 1$  meter.

For the NLOS paths, because of the second consideration in the last subsection, their length will be bounded within  $d_1$  and  $2d_1$ , i.e.,  $d_1 < d_i < 2d_1$ ,  $i = 2, \dots, n$ . By the physical laws of the radio reflections, we have  $\Gamma < 0.3$  for NLOS paths.

### E. Summary of the Treatments

With all these treatment techniques, the conditioning of the CFP will be great improved. In general, the parameter  $c$  is a given number no more than 0.1. By practical deployments the path lengths are no less than 1 meter (transmitters are deployed on the ceiling). For the single path scenarios, the condition number (8) is no more than  $(9 \times 0.1^2 + 2)^2 < 5$  which can be considered as well-conditioned. For multiple paths, because of the reflection co-efficiency  $\Gamma$ , the LOS path energy will be the dominance factor and thus the condition number will also be restrained to an acceptable level.

## VI. EXPERIMENT

Integrating all these treatments, we implement a RSS-based tracking system called MuD. In this section, we first introduce the architecture and implementation of MuD, followed by the performance evaluation. Notice that all our experiments are conducted in dynamic environments by default where several people (typically five) are free to move around in the room.

### A. Architecture of MUD Tracking System

MuD has three major steps in Fig. 5. First, it derives the hardware-dependent parameter  $c$  by any of the three proposed methods in Sec.5.2, (i.e., specifications, chamber or online training). In the run-time, a number of anchors with given positions will function as the receivers to receive beacon messages from the target node (transmitter). Anchor nodes collect the RSS measurements, alter their channels of the measurements (transmitter will also alter) and deliver the measurement results to a central server. The server will apply a trilateration algorithm and display the results. Typically, the first step conducts only once while the later two steps will keep operating to provide continuous locations of the target.

### B. Implementations of MUD Tracking System

We implement MuD tracking system based on TelosB sensor platform [1] because of its low cost, easy implementation and convenient deployments. The MuD is deployed at the  $20 \times 20m^2$  laboratory with three anchor nodes at the corner of the ceiling. A snapshot of the system layout is depicted in Fig. 6. By the 802.15.4 standard TelosB sensors have 16 channels and channels are spaced by  $5MHz$ . The wavelengths of these radio waves are on the order of centimeter. The transmission power is fixed at  $-10dBm$ . All the anchors nodes are merely the receivers and simply receive the beacon messages. The target node is the only transmitter sending out beacon messages. Each transmitter stays in one channel for about  $50ms$  to send out beacons. We perform synchronization for all the nodes by the reference-broadcast method [8].

When the anchor nodes receive packets, it means the target enters the system. They will immediately transmit the data back to the server. To reduce unnecessary wireless traffic and radio interference, anchor nodes are connected to the server through USB cables. As long as the transmission is over, transmitters and receivers will switch to a new channel. When all the channels have been visited once, the server begins its

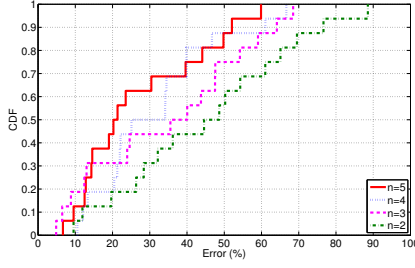


Fig. 7. Accuracy of individual ranging with different path number (CDF)

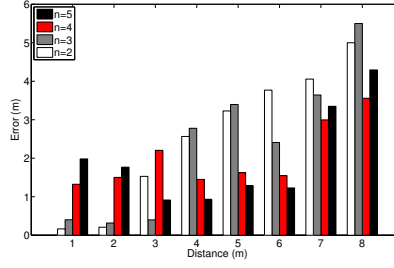


Fig. 8. Accuracy of individual ranging with different path number

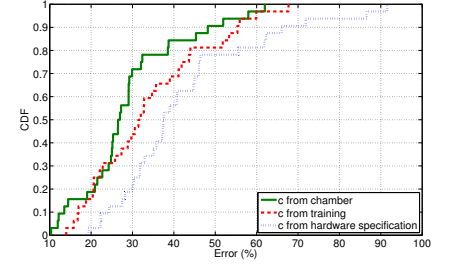


Fig. 9. Accuracy of individual ranging with different  $c$  (CDF)

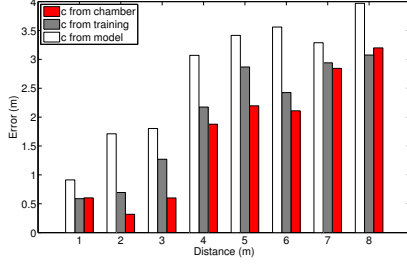


Fig. 10. Accuracy of individual ranging with different  $c$

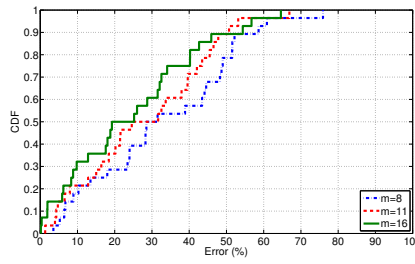


Fig. 11. Accuracy of individual ranging with different channel number (CDF)

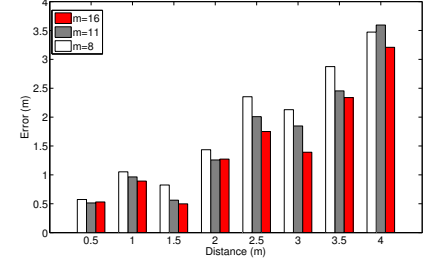


Fig. 12. Accuracy of individual ranging with different channel number

computation. After the ranging for each anchor to the target, trilateration localization [18] is applied to achieve the target location on the ground. Traditional RSS-based localization technologies rarely use trilateration, since they are hardly to realize accurate ranging between two nodes. Applying MuD into trilateration is able to verify that the MuD method can realize accurate ranging without high cost, laborious training or other environmental limitations.

### C. The Impact of Assumed Multipath Number

At first, we investigate the impacts of the number of paths  $n$  on the ranging accuracy. Based on a fixed pair of sensors, we conduct experiments under 32 different distances ranging from  $1m$  to  $8m$  with  $0.25m$  apart. In the analysis, the number of paths  $n$  varies from 2 to 5. The parameter  $c$  is obtained by online training. The initial value of  $d_1$  is set as 1 and the other initial values are set according to Sec. 4.4. Fig. 7 shows the cumulative density function (CDF) of normalized errors in percentage and Fig. 8 gives the absolute errors. In general, we find  $n = 5$  outperforms the other settings with over 65% of ranging having the ranging error less than 20%. When  $n > 4$ , the accuracy improvement is marginal. The reason is that in practice we have no knowledge of  $n$  and can only make assumption on it to carry out the analysis. A high  $n$  will introduce more variables to the model function  $P(x, \lambda)$ , which will take the risk that the problem becomes ill-conditioned during the computation. In addition, when the node distance is very short (e.g., less than  $2m$ ), lower  $n$  will have a relative higher accuracy. It may because in that scenario the actual number of paths is small too. Considering all these factors we set  $n = 4$  in our later experiments.

### D. The Impact of $c$

In this set of experiments we evaluate the different approaches to obtain the fixed unknown  $c$ , i.e. by hardware specifications, from chamber and from training. The experiment setting is the same as the above except  $n = 4$ . The comparison results are shown in Fig. 9 and Fig. 10. Fig. 9 is the CDF of on the normalized errors from all samples, and Fig. 10 shows the absolute errors. We may see that the hardware specification approach performs the worst among others. Its average error is about 40%. We believe it is mainly due to the hardware derivation on this parameter. Not surprisingly, the chamber training approach performs the best accuracy (about 25%). We also find that the online training approach exhibits a similar performance as the ideal chamber training. The average error is about 30%. Compared with the chamber approach, the performance loss is only 5%. In our later experiment, we apply the online training approach because of the practical concerns.

### E. The Impact of Used Channel Numbers

Fig. 11 compares the normalized ranging accuracy with different channel numbers  $m = 8, 11, 16$  respectively. The absolute values are shown in Fig. 12. We set  $n = 4$ , take the online training approach and the other settings are the same as above. We find that,  $m = 8$  has the averaged range error about 32%. When we use the maximum number of channels 16, the accuracy is the best 26% in average. With these, we suggest more channels when they are available when latency and measurement overhead are not the concern.

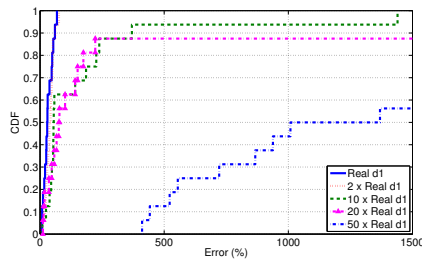


Fig. 13. Accuracy of individual ranging with different initial value

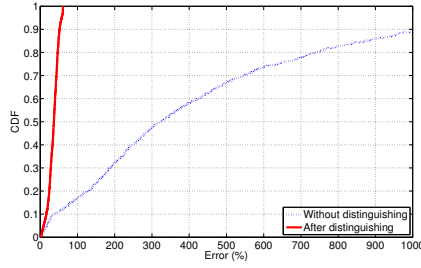


Fig. 14. Accuracy comparison without/after filtering out multipath effect

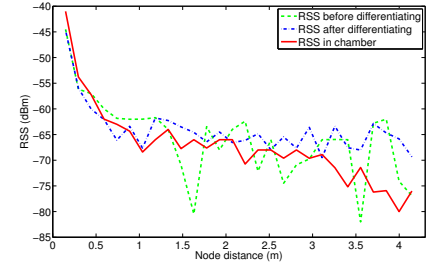


Fig. 15. RSS results before/after differentiating

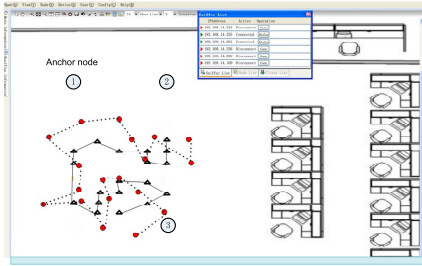


Fig. 16. Tracking example

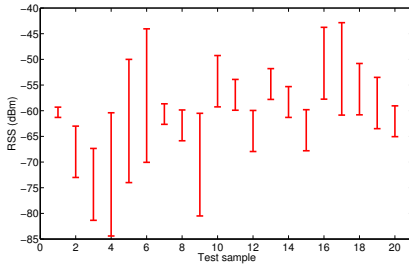


Fig. 17. RSS variance in dynamic environment

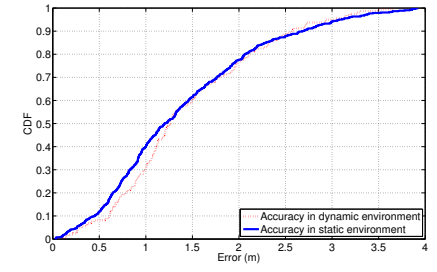


Fig. 18. Tracking error in dynamic environment

#### F. The Impact of Initial Value Setting in MuD

Initial value setting for iterations will also affect the final performance. We test different setting on LOS path length ( $d_i$ ). The initial values of others will also be changed according to  $d_1$ . The other experimental settings are suggested as above experiments. As shown in Fig. 13, the initial values have the great impact on the accuracy. Especially when the initial value is very large, e.g., 50 times of the real sensor distance. Only when the initial value is set in a reasonable range (say several times of the real distance), a reasonable solutions is expected. These confirms the importance of the online training. We should continuously track the target so that a reasonable guess of the solutions can be set as the initial setting. Each time, we choose to use the previous tracking result as the initial value of current input in the real scenario. As the target has limited mobility indoors, this guess will be close to the real one. The impact of initial value setting will be effectively alleviated. How to get a reasonable guess with no any pre-knowledge of the target is left for future work.

#### G. Accuracy

To comprehensively investigate our method for individual ranging, we conduct experiments between 20 pairs of nodes with 500 sample distances. As shown in Fig. 14, by traditional ranging-based technology [17] (mapping the RSS information to distance directly), the average ranging errors is around 300%. By our method, the average errors decreases to about 30%. The improvement is up to 10 times. To explain how it happens, Fig. 15 shows the RSS behaves before and after distinguishing the multipath signals. We find that, before distinguishing, the RSS curve fluctuates dramatically with the distance due to the multipath effect. But after distinguishing,

the multipath effects are successfully filtered out and the residual RSS from the LOS path becomes much smoother. It decreases nearly monotonically as the distance increases. Such results are much similar to the experimental results in chamber where multipath effect is not obvious. As Fig. 15 shows, the difference between RSS after distinguishing and ideal RSS in chamber is only about 10%. We also evaluate the accuracy of the MuD tracking system (trilateration on the previous ranging results). In our experiments, we let a person carry the target sensor with walking speed about  $2m/s$ . Fig. 16 shows an example by the MuD. The solid line is the real trace and the dashed line is the estimated one. We test 100 different target traces on the ground. The average error is about  $1m$ .

#### H. Latency of MuD Tracking System

In the MuD tracking system, the latency depends on how much time for each sensor to sweep over all the channels. In our scenario, we have 16 channels. At each channel, one packet is transmitted. Each TelosB sensor node takes  $7ms$  average to transmit a packet of 51 bytes [1]. But in order to avoid beacon collision if multiple object scenarios, we prolong the data transmission time to  $50ms$ . The transmitter can randomly transmit the packet within this time. The Channel switching is about  $0.34ms$ . The other data transmission time through wire connection and computation time can be neglected. As a result, for each sensor node to finish switching all the sensor nodes should be  $(50 + 0.34) \times 16 \approx 0.8s$ . In summary, our system can reach the real time tracking latency to as fast as  $0.8s$ . Lower latency is expected with smaller measurement time.

#### I. Comparison with Static Environment

We compare the results in both dynamic and static environments, based on 20 target locations on the ground (Fig. 6).



In the static environment, no one is allowed to move. In the dynamic environment, the walking people around will change their position after RSS measurement over all the channels. they cause the RSS to vary dramatically as shown in Fig. 17. The largest RSS difference among the test samples is up to 25dB. Fig. 18 shows the accuracy of MuD in the two environments. We can see that, as the multipath induced by the moving people are successfully filtered out, the accuracy in the dynamic environment is quite similar to the accuracy in the static environment. They both have averaged error about 1 meter. The difference between them is less than 5%. Such result confirms that MuD is robust to the environment changes.

## VII. RELATED WORK

Most existing RSS-based ranging works try to find appropriate mapping between RSS and corresponding distance. For example, RADAR [2] built a radio map for the environment and referred to the map during localization. LANDMARC [13] localized nodes by finding some reference nodes who have similar RSS value with the target nodes. It requires dense deployment of nodes. All these approaches are essential profile-based (build a RSS profile for the environment, and refer it later). The critical assumption is the RSS profile will not change. In dynamic environments, however, this assumption is not true as new radio propagation paths may appear and existing paths may fade, causing the profile to change significantly. It is noted that, although RIPS and related systems [12], [11], [4] can offer accurate ranging between two nodes, they still suffer from the multipath environments especial indoors.

Besides these deterministic approaches, probabilistic ones are also proposed (e.g., Horus [19], [9]). In these approaches, a probabilistic model is constructed to represent the behavior of the link RSS values. We argue, however, the variance of the RSS values is not probabilistic. When the multi-path effects are correctly identified, RSS of wireless links are deterministic.

Rallapalli et.al [15] noticed the frequency diversity of RSS measurement but simply used the average to represent the RSS. In fact, all the RSS values at the different frequencies are correct. The difference exists because the changed constructive/destructive relations between signals from different paths. That difference is not due to the measurement errors. Noticing this, we use equations to explore such relations and get a better understanding of the multi-path effects.

In communication community, multipath effects have also been studied. A multi-carrier technology [6] use OFDM [5] to extract the phase information of the radio wave. It however needs the physical layer information and the cost is high, which are not suitable for commodity hardware.

## VIII. CONCLUSION

In this paper, we study the multi-path phenomenon in RSS-based ranging and localizations. We propose to exploit the frequency diversity of the radio propagation paths to mine the phase information of the radio paths. As such, the signal amplitude of the LOS path can be identified. Rely only on the RSS measurements we can accurately ranging (localize)

nodes in dynamic environments with severe multipath effects. Experimental results show that the ranging and localization errors are 1m in average in a 20m×20m laboratory. Compared with traditional RSS-based ranging approaches in dynamic environment, the improvement is up to 10 times. In the future, we will address the external radio interference issue when the interference is light. We will also study the scenarios when LOS path does not exist. At last, we will investigate techniques to accommodate changes of the environments during the RSS measurements, assuming that change exists but not significant.

## ACKNOWLEDGEMENT

This research was supported in part by Hong Kong RGC Grants HKUST617710 and HKUST617811, National High Technology Research and Development (863) Program of China under Grant No. 2011AA010500, National Science and Technology Supporting Program under Grant No. 2012BAH07B00, China NSFC Grants 60933011, 61170077, 61073180, 61170247, 61003272 and 61103001, the SZ-HK Innovation Circle Project under Grant ZYB200907060012A, China NSFGD Grant 10351806001000000 and the Science and Technology Project of Shenzhen JC200903120046A.

## REFERENCES

- [1] <http://www.xbow.com/products/productdetails.aspx?sid=252>. XBOW Corporation TelosB mote specifications.
- [2] P. Bahl and V. N. Padmanabhan. Radar: an inbuilding rf-based user location and tracking system. In *Proceedings of IEEE InfoCom*, 2000.
- [3] C. A. Balanis. Antenna theory: Analysis and design. In *2d Ed*, Wiley: New York, NY, 1997.
- [4] H. Chang, J. Tian, T. Lai, H. Chu, and P. Huang. Spinning beacons for precise indoor localization. In *Proceedings of ACM SenSys*, 2009.
- [5] S. Coleri, M. Ergen, A. Puri, and A. Bahai. Channel estimation techniques based on pilot arrangement in ofdm systems. In *IEEE Transactions on Broadcasting*, 2002.
- [6] D. Cyganski, J. Orr, and W. R. Michalson. A multi-carrier technique for precision geolocation for indoor/multipath environments. In *Proceedings of IEEE ION*, 2006.
- [7] J. J. E. Dennis and R. B. Schnabel. *Numerical Methods for Unconstrained Optimization and Nonlinear Equations*. 1996.
- [8] J. Elson, L. Girod, and D. Estrin. Fine-grained network time synchronization using reference broadcasts. In *Proceedings of OSDI*, 2002.
- [9] A. Haeblerlen, E. Flannery, A. M. Ladd, A. Rudys, D. S. Wallach, and L. E. Kavasaki. Practical robust localization over large-scale 802.11 wireless networks. In *Proceedings of ACM MobiCom*, 2004.
- [10] S. N. Jaspersion and S. E. Schnatterly. An improved method for high reflectivity ellipsometry based on a new polarization modulation technique. In *Review of Scientific Instruments*, 1969.
- [11] B. Kusy, A. Ledeczki, and X. Koutsoukos. Tracking mobile nodes using rf doppler shifts. In *Proceedings of ACM SenSys*, 2007.
- [12] M. Maroti, B. Kusy, G. Balogh, P. Volgyesi, A. Nadas, K. Molnar, S. Dora, and A. Ledeczki. Radio interferometric geolocation. In *Proceedings of ACM SenSys*, 2005.
- [13] L. M. Ni, Y. Liu, Y. C. Lau, and A. P. Patil. Landmarc: Indoor location sensing using active rfid. In *Proceedings of IEEE PerCom*, 2003.
- [14] D. Pozar. Microwave engineering. In *Proceedings of 2nd ed.*, John Wiley and Sons, Inc., 1998.
- [15] P. Sharma and S. Tripathi. Node localization using received signal statistics. In *Proceedings of IEEE MASS*, 2005.
- [16] E. Z. W. N. Systems. Design with an inverted-f pcb antenna.
- [17] K. Whitehouse, C. Karlof, and D. Culler. A practical evaluation of radio signal strength for ranging-based localization. In *Proceedings of ACM SIGMOBILE*, 2007.
- [18] Z. Yang and Y. Liu. Quality of trilateration: Confidence-based iterative localization. In *Proceedings of IEEE TPDS*, 2010.
- [19] M. Youssef and A. Agrawala. The horus wlan location determination system. In *Proceedings of ACM MobiSys*, 2005.